ENERGY LOSS IN MEMS RESONATORS AND THE IMPACT ON INERTIAL AND RF DEVICES

Marc Weinberg[1], Rob Candler[3], Saurabh Chandorkar[2], Jonathan Varsanik[4], Thomas Kenny[2], Amy Duwel[1]
[(1)]Charles Stark Draper Laboratory, Cambridge, MA
[(2)]Department of Mechanical Engineering, Stanford University
[(3)]Department of Electrical Engineering, University of California Los Angeles
[(4)]Department of Electrical Engineering and Computer Science, Massachusetts Institute of Technology

ABSTRACT
In this paper, we review the current understanding of energy loss mechanisms in micromachined (MEMS and NEMS) devices. We describe the importance of high quality factor (Q) to the performance of MEMS gyros and MEMS resonators used in radio-frequency applications.

INTRODUCTION
Dissipation in mechanical resonators has been of significant interest to the scientific and engineering communities since the early 1950's. Driving applications at that time included crystal radios and gravitational wave detectors. More than fifty years later, we continue to refine our understanding of dissipation mechanisms, still motivated by a demand for low-loss resonators in frequency selection, timing, and sensing applications. Over this time, the engineering technology for fabricating and integrating these devices into electronic systems has evolved dramatically. However, the fundamental physics described during the 1950's and 1960's continues to guide engineering practice today. New insights have been published based on application-specific designs and advanced fabrication technologies. In 1976, Nowick and Berry[1] contributed a comprehensive text that still covers every internal dissipation mechanism known today. In 1985, Braginsky [2] thoroughly reviewed internal loss as well as external factors such as air and support loss. The rapid advancement of micromachining technologies in the 1980's and 1990's motivated a fresh review of mechanical dissipation, as the relative significance of various dissipation channels depends sensitively on overall device size and integration. Yasumura's paper in 2000 [3] offered the community a valuable discussion on size effects specific to MEMS devices. Nearly a decade later, new insights and modeling tools are enabling micro- and nano-resonators with performance matching or exceeding that of macro-scale devices. This paper presents an updated review of energy loss mechanisms in mechanical resonators, with particular emphasis on the impact of dissipation in two major application areas – gyros and radio-frequency resonators.

MECHANISMS OF DISSIPATION
In most treatments of mechanical dissipation, the device is modeled as a linear harmonic oscillator whose eigenfrequencies and mode shapes can be found analytically or numerically. To first order, for a given mode amplitude:

$$\ddot{x} + 2\beta\dot{x} \ + \omega_o^2 x = F_n \qquad (1)$$

where ω_o is the modal frequency and F_n is the mass normalized external modal force. The loss term β is related to the modal Quality factor (Q) by $Q = \omega_o/2\beta$. The losses from various mechanisms are treated as dampers in parallel so that the total Q is calculated by summing over each of *i* loss mechanisms:

$$Q_{tot}^{-1} = \sum_i Q_i^{-1} \qquad (2)$$

Table 1 summarizes results, analysis and modeling tools available for the major energy loss mechanisms relevant to MEMS devices. Some of the effects not specifically covered in this review include bulk dislocation and defect damping, surface roughness, as well as interface effects in composite structures.

Thermal Energy Loss
The thermal bath in solids is composed of quanta of vibrations called phonons. It is expected that a micro/nano mechanical resonator that involves periodic straining of a solid may lose energy from the fundamental vibration mode of the resonator to the thermal bath via phonon interaction. Strain in solids results in a change in the modal frequencies of phonons due to anharmonicity (non-linearity) in interatomic interaction forces [4-6]. As a consequence, the equilibrium phonon population is disturbed and phonons interact with each other in an effort to push back the populations to Bose-Einstein equilibrium. If the resonator's period of oscillation is much smaller than that of the phonon relaxation time (typically ~ 100ps), the equilibrium is attained and the temperature changes locally. Therefore, non-uniformity in the strain field causes temperature gradients in the solid, and an associated heat transfer; the resulting energy loss is known as thermoelastic dissipation (TED). Zener identified this effect and derived a formula for fixed-free beam using a classical picture of thermodynamics [7, 8]. Certain resonator geometries such as square Lamé mode, torsional mode and contour mode of a ring have been shown to be immune to TED due to lack of significant strain gradients [9].

If, on the other hand, the period of oscillation of the resonator is small enough and the resonator material is dielectric in nature, the upper limit to quality factor is set

by a quantum effect called Akhieser effect (AKE) [10]. The small period of oscillation restricts the ability of phonons to reach full equilibrium. The non-equilibrium state of phonons and the fact that the anharmonicity for each phonon mode characterized by mode Grüneisen parameter (γ_{ks}) is different leads to irreversible generation of entropy during this process [4]. Chandorkar *et al.* [11] derived a formula for quality factor of AKE-limited mechanical resonators. The most important characteristic of this formula is that it is solely dependent on material properties.

TED has been understood to a great extent as far as the standard micro/nano mechanical resonators are concerned. Some of the relatively unchartered areas in this field are: temperature gradient effects on thermoelastic dissipation[12], subharmonic actuation of the micromechanical resonators with TED limited Q [13] and effect of TED on noise in resonators. AKE needs to be explored further. Presently, one of the most significant difficulties in using the formula for AKE is the lack of sufficient data on the material properties. Standard resonator geometries that can achieve Qs in the vicinity of the AKE limit should be used to characterize these properties further.

Support Losses

In physically realizable devices, acoustic energy is not perfectly reflected at the resonator's boundaries but can radiate into the supporting substrate, lowering the resonator Q. To model radiation effects, the boundary must perfectly absorb incoming waves from all angles without reflections. This is achieved through a perfectly matched layer (PML) at the model's boundary. Surprisingly, this capability was only recently introduced in mechanical modeling tools, pioneered by Bindel [14]. It is now available in the forced-response solver of CMOSOL [15]. In reference [16] a more numerically efficient matched layer (ML) eigenvalue analysis is introduced and the error is quantified for the problem of interest.

Wave-guiding and impedance matching principles motivated great experimental progress in high Q design. After early implementation of quarter wave transformer-based isolation in [17], the parameter space was later fully explored by [18]. However, it can be a challenge to identify which types of waves are excited in a given support-resonator configuration. For example, the BAW community saw a significant Q improvement once it was realized that shear waves were generated in the substrate [19]. High isolation based on material impedance mis-matching has also been employed since the early SAW and BAW devices. In an elegant micro-resonator implementation, the support of a contour-mode diamond disk was made from polysilicon [20]. Energy trapping approaches [21] familiar in quartz devices are harder to implement at MEMS scales. However [22] shows that the mode itself can be isolated by design. Others have considered designing SAW-type Bragg reflectors into the substrate surrounding the resonator. A simple mesa structure for energy localization has also proven effective [23].

Analytical calculations for radiation losses are available in a few simple cases. All analyses assume a weak coupling limit, where the resonator mode and frequency are found under the assumption of a perfectly reflecting boundary. The resulting stress or displacement at the boundary is treated as a source input to the semi-infinite substrate. The substrate impedance is needed for calculating the power dissipation and depends on the geometry of its connection to the resonator. Park [24, 25] offered a semi-analytic approach where a calculated substrate impedance was coupled to an FEA model for the resonator. Cross and Lifshitz assumed a finite resonator/substrate boundary in 2D [26] to obtain analytic Q values for several different cantilever modes. In [27] a lucid analysis of the cantilever in 2D matched well to [26] and set the stage for a more the complicated case of a vibrating disk [28]. Judge *et al* [29] considered the limit where the resonator is a point source and addressed a challenging 3D geometry. It would be illuminating to see more comparisons of analytical and numerical predictions, since a single loss mechanism can be isolated. An initial comparison for the case of a contour mode disk is provided in [16].

Fluid Loss

Damping effects are generally divided into shear or Couette damping where the velocity V_x is parallel to the substrates and moving plates and squeeze film where the velocity V_z is normal to the plates or the rotation ω_y is parallel to the surfaces (Figure 1). For shear motion, the damping force is approximately [30, 31]:

$$F_x \approx \frac{\mu A}{g+2\lambda} V_x \tag{3}$$

where A = plate area, μ = gas viscosity, g = air gap, λ = mean free path (0.06 μm at atmospheric pressure and inversely proportional to pressure. For squeeze translation, damping is of the form [31-35]:

$$F_z \approx \frac{\mu L^4}{g^2(g+6\lambda)} V_z \tag{4}$$

where L represents characteristic plate dimensions (a or b in Figure 1). The effects of mean free path and pressure on damping have been derived by slip [31] and molecular flow considerations [36-38] and experimentally verified [31]. For MEMS devices run at atmospheric pressure, gas damping is generally the dominant loss mechanism. For 1 mTorr pressure levels achieved in small packages, the shear damping is generally smaller than other effects such as thermoelastic damping Because of the dependencies

on gap, squeeze damping is usually much larger than the shear terms. For squeeze film without perforations or pressure relief holes, gas damping dominates even in a relatively high vacuum. With perforation and evacuation, gas damping is similar in magnitude to other damping sources. For squeeze film damping without perforations, fluid inertia appears in the higher frequency response [34-38]. For all gas damping situations, the gas' added stiffness [39] should be considered.

For damping without a cover plate, [40] derives conditions for which fluid waves can radiate to the far field and greatly increase damping in flexural plate wave devices. For a long thin plate or cantilever (b<<a in Figure 1) operating at low frequencies in air, the damping force is approximately [41],

$$F_z \approx \mu b V_z \tag{5}$$

Extensions of [42] using slip boundary conditions indicate that this damping does not depend on mean free path. [43] employed molecular flow, assumed wide plates, and concluded that damping was proportional to width and ambient pressure. The important difference between [41] and [43] is the relation between the diffusion distance and the plate width. For wide plates, the diffusion distance is determined by gas parameters [44] while for narrow beams and low frequencies the diffusion distance is determined by the beam width.

Electrical Damping

Electrical stimulation and readout techniques are commonly used with RF and inertial MEMS, to interface MEMS with the control and measurement circuit.

Electrical damping has been proposed as a beneficial technique in accelerometers [45], to effect quicker response time. Consider one end of a variable capacitor (C) connected to a resistor (R) and voltage source (V). As the capacitance changes, the resistor modifies the voltage across the capacitor. The damping force (F_z) is described by:

$$\frac{F_z}{V_z} = R\left(\frac{\partial C}{\partial z}\right)^2 V^2 \tag{6}$$

where V_z is the resonator velocity. Finite gain in transimpedance amplifiers causes the virtual ground to differ from true zero and to dissipate energy.

In resonators, differential measurements have been used to mitigate electrical damping. In [46], the SiC resistivity caused electrical damping. With differential readout there are smaller electrical currents and, hence, smaller Ohmic loss; thus, the Q was increased by an order of magnitude.

Also, a ring-down approach can be used to reduce electric damping. For this measurement, the device is driven into resonance and then all stimulus and measurement are turned off. The sensing is only periodically sampled as the device rings down, allowing for a reconstruction of the decay envelope while minimizing electric damping.

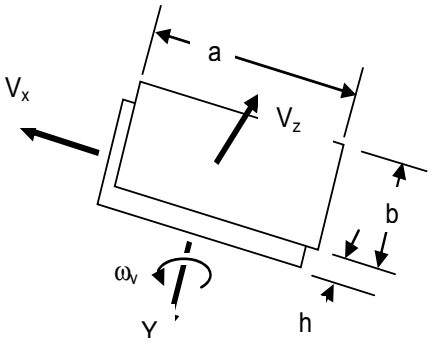

***Figure 1**: Nomenclature for damping between plates*

Surface Effects

Several research groups have identified an important scaling trend in the measured dissipation, in that the Q values decrease as surface-to-volume ratios increase [3, 47-49]. In particular, the Q of very thin cantilevers has been found to scale linearly with resonator thickness, and this scaling behavior is used to experimentally identify surface-loss dominated structures.

The roles of adsorbed species and surface coatings in energy loss have been explored by a number of groups, with an emphasis on the positive impact that thermal annealing has on Q. Henry *et al* [50] and Mohanty *et al* [51] offer the hypothesis that a dominant mechanism is the loss due to coupling to electronic defects on the silicon surface. References [50, 52] support this with experiments using non-oxide coatings that vary the electronic defects at the interface. In addition, the proposed importance of electrical passivation properties makes sense of what appear to conflicting results in the literature: the fact that a thermal oxide improved Q [53], while deposited, chemical, and even native oxides have been linked to increased dissipation [49, 54-56].

Building on early work in amorphous crystalline solids [57], Mohanty *et al* [51] provide a two-level system model for surface dissipation due to electronic defects. More recent work [58] provides a deep discussion of the two-level system model for dissipation in the low-temperature regime.

Other reconfiguration-based mechanisms that might contribute to surface damping have been proposed, though detailed experimental studies have been limited. These include grain re-orientation and movement of defects that do not necessarily contribute electronic energy levels. Static mechanisms that have been explored include increased phonon scattering at rough boundaries (an extension of Akhieser damping) [59], and thermoelastic damping across grains in surface films (also a volume effect for polycrystalline resonators) [1, 2].

IMPACT OF Q ON DEVICE PERFORMANCE

MEMS Gyros

The moving mechanism for a MEMS gyro is shown in Figure 2. There are gyros with other arrangements of axes [60, 61] but the physics is similar. For high performance MEMS tuning fork angular rate sensors, damping and fluid effects require package evacuation [62]. Even with evacuation (typically to 1-10 mTorr), other damping mechanisms limit performance [62]. For evacuated MEMS gyros, the drive (parallel to the substrate) and sense axis damping varies by a factor of 2-3 over the desired operating range of -40 to +85°C. Thermoelastic damping and temperature sensitive material properties are likely causes for the damping variation over temperature. The gyro drive axis is generally operated at resonance and drive forces are electrostatically coupled into the sense direction. Because these drive forces (proportional to damping) are comparable to the desired Coriolis forces, damping variation and its repeatability becomes an important error source [62].

Successful demodulation of Coriolis induced motion and rejection of undesired quadrature motion [62] depend on the phase between drive and sense axes motion. Therefore, sensor performance depends on low and repeatable sense axis damping.

Drive motion as in Figure 2 can result in hydrodynamic forces (surf boarding) in the sense direction. Evacuation and perforations (damping relief holes) mitigate the gyro bias errors below those of electrostatic coupling [62]. For mode matched gyros, the scale factor can depend on Q or Q^2 (depending on control loops) causing more errors.

RF Resonators

Understanding Q is a critical step toward commercialization of RF resonators or narrow bandwidth filters. For example, the Q can impact the near carrier phase noise [63] and power handling [64], both important parameters for use of resonators in communications. Also, the mass-spring-damper mechanical system of a resonator can be modeled in its simplest form as an equivalent L-C-R circuit. The equivalent resistance, R, is dependent upon the quality factor in both capacitive [65, 66] and piezoelectric [21] devices. Understanding Q, and therefore R, is important for several reasons: (1) Q can be increased (and R reduced) with design techniques that result from understanding of energy dissipation mechanisms, resulting in easier design of interface circuits. Reduction in R allows for reduced power in the sustaining circuit and lower drive and bias voltages; (2) The ability to *predict* the Q of a structure is useful in that it enables simultaneous design of interface circuits without waiting for experimental results from a MEMS fabrication cycle; (3) The equivalent resistance from the resonator can be a source of Johnson noise [65].

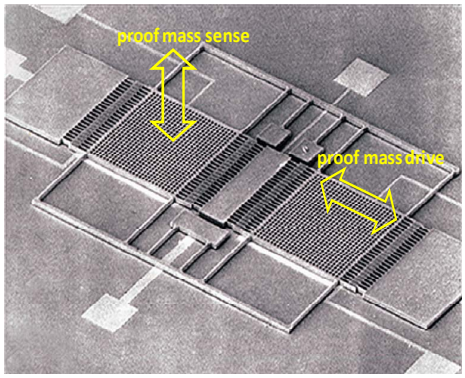

***Figure 2**: Draper tuning fork gyro, with drive and sense mode motions indicated by arrows.*

CONCLUSIONS

The past decade has delivered great progress in the understanding of fundamental dissipation processes in MEMS/NEMS resonators. Though many basic mechanisms were identified in the early days of radio, outstanding recent contributions have been in advanced numerical tools and insightful analytical modeling. The demand for high Q resonators in MEMS gyro and RF communications applications continues to motivate fundamental research in mechanical energy dissipation.

Effect	Experimental systems studied	Numerical models available	Analytical models available	Cantilever formula[i]
Thermo-elastic	• Fixed-fixed beam (flexural) [67, 68] • Fixed-fixed beam (extensional)[69] • Ring (wine glass mode)[70] • Paddles [71]	• Comsol eigenfrequency or forced response [15, 72] • Custom [72] • Ansys forced response [73]	• Fixed-fixed beam [74] • Disk breathing [9] • Thickness mode [9] • Contour mode [9] • Composites [75, 76]	[1, 7, 8, 74]: $Q = \frac{C_v}{E\alpha^2 T}\frac{1+(\omega\tau_{ted})^2}{\omega\tau_{ted}}$ $\tau_{ted} = \frac{t^2\rho C_{sp}}{K}$
Akhieser	• Disk (contour mode) [77, 78] • Square (Lamé mode) [79] • Bar (longitudinal harmonic) [80]		• All mechanical resonators [11]	[2, 11]: $Q = \frac{3\rho c^2}{2\pi\gamma^2 C_v T}\frac{1+(\omega\tau_{ph})^2}{(\omega\tau_{ph})}$
Support Loss	• Paddles [22] • Cantilevers [18, 29] • Contour disks [14, 16, 23, 28, 81]	• HiQ Lab PML[14] • Comsol PML forced response [16] • Comsol ML eigenfrequency or forced [16] • Semianalytic [24, 25]	• Cantilever flexural mode [26, 27, 29] • Contour mode disk [28]	In plane [26, 27]: $Q \sim (L/w)^3$ Out of plane [26, 29, 82]: $Q \sim (L/w)(h/t)^2$ Out of plane, thick substrate [29]: $Q \sim (L/w)(L/t)^4$
Fluid Loss	• Shear plates [30, 31] • Perforated and solid paddles [31, 34, 35] • Cantilevers [41, 83]	• Compressible, Reynolds: [31, 84] • Incompressible Navier-Stokes: FastStokes [85], FEA of Poisson's equation [86] • Molecular dynamics code [43, 87]	• Incompressible: shear against unbounded fluid [44, 88]. • Compressible: shear against bounded fluid [44, 88], squeeze film [32-35, 84, 88, 89] • Molecular: unbounded fluid [83, 87, 90, 91]	Molecular regime, limit of wide plates [43, 92]: $Q \sim (t/L)^2 / P_o$ Incompressible unbounded fluid [41, 93]: $Q \sim t^2 w/(\mu L^2)$ Incompressible squeeze film [93]: $Q \sim \left(\frac{t}{wL}\right)^2 \frac{g^3}{\mu}$
Surface Loss	• Oxide coatings [3, 53] • Annealing & Thermal [3, 49, 51, 53, 94-96] • Time dependence [94] • Field dependence [51] • Surface chemistry variations [52]		• Cantilever surface with complex modulus [3] • Intercrystalline thermal currents [1, 2]	General [3]: $Q = \frac{wt}{2\delta(3w+t)}\frac{E}{E_{sl}}$ Intercrystalline thermal (contour mode vibration) [1, 2]: $Q \sim \frac{t}{4\delta}\frac{C_p}{E\alpha^2 T}\frac{1+(\omega\tau_s)^2}{\omega\tau_s}$
Electrical	• Differential Measurement [46] • Accelerometer Damping [45]		• Differential Measurement [46] • Capacitive readout [2, 97]	Capacitive readout through finite gain amplifier[(i)][97]: $Q = \frac{mC_f\lvert A_g\rvert\omega^2}{2V_B^2(dC/dz)^2}$

Table 1*: Summary of loss mechanisms and published results in each category. If available, a formula is provided for the Q of a cantilever vibrating in flexural mode out of the plane of the wafer, at frequency ω, where Q is related to damping constant in N-s/m by: $\sqrt{E\rho}t^2 w/(QL)$. See endnote (i) for details regarding the cantilever dimensions, physical constants, and other variables used in the Q formulas.*

REFERENCES

[1] A. S. Nowick and B. S. Berry, *Analastic Relaxation in Crystalline Solids*: Academic Press, 1972.

[2] V. B. Braginsky, V. P. Mitrofanov, and V. I. Panov, *Systems with Small Dissipation*: The University of Chicago Press, 1985.

[3] K. Yasumura, T. Stowe, E. Chow, T. Pfafman, T. W. Kenny, B. Stipe, and D. Rugar, *IEEE JMEMS,* vol. 9, p. 117, 2000.

[4] T. O. Woodruff and H. Ehrenreich, *Physical Review,* vol. 123, p. 1553, 1961.

[5] H. H. Barrett and M. G. Holland, *Physical Review B,* vol. 1, p. 2538, 1970.

[6] H. E. Bömmel and K. Dransfeld, *Physical Review,* vol. 117, p. 1245, 1960.

[7] C. Zener, *Physical Review,* vol. 52, p. 230, 1937.

[8] C. Zener, *Physical Review,* vol. 53, p. 90, 1938.

[9] S. Chandorkar, R. N. Candler, A. Duwel, R. Melamud, M. Agarwal, K. E. Goodson, and T. W. Kenny, *Journal of Applied Physics,* vol. 105, p. 043505, 2009.

[10] A. Akhieser, *J. Phys. (Akademiia Nauk-Leningrad),* vol. 1, pp. 277-287, 1939.

[11] S. A. Chandorkar, M. Agarwal, R. Melamud, R. N. Candler, K. E. Goodson, and T. W. Kenny, in *IEEE 21st International Conference on MEMS*, 2008, pp. 74-77.

[12] S. A. Chandorkar, H. Mehta, M. Agarwal, M. A. Hopcroft, C. M. Jha, R. N. Candler, G. Yama, G. Bahl, B. Kim, R. Melamud, K. E. Goodson, and T. W. Kenny, in *Micro Electro Mechanical Systems, 2007. MEMS. IEEE 20th International Conference on*, 2007, pp. 211-214.

[13] S. K. De and N. R. Aluru, *Physical Review B (Condensed Matter and Materials Physics),* vol. 74, pp. 144305-13, 2006.

[14] D. Bindel, E. Quévy, T. Koyama, S. Govindjee, J. Demmel, and R. T. Howe, in *IEEE 18th International Conference on MEMS*, Miami, FL, 2005.

[15] "COMSOL MULTIPHYSICS®," 3.4 ed.

[16] P. G. Steeneken, J. Ruigork, S. Kang, J. van Beek, J. Bontemps, and J. J. Koning, "Parameter Extraction and Support-Loss in MEMS Resonators," in *COMSOL Users Conference 2007* Grenoble, 2007.

[17] K. Wang, Y. Yu, A. Wong, and C. T. C. Nguyen, in *IEEE 12th International Conference on MEMS*, Orlando, FL, 1999, pp. 453-458.

[18] A. Ferguson, L. Li, V. Nagaraj, B. Balachandran, B. Piekarski, and D. DeVoe, *Sensors and Actuators A,* vol. 118, pp. 63-69, 2005.

[19] S. Marksteiner, J. Kaitila, G. Fattinger, and R. Aigner, in *IEEE Ultrasonics Symposium*, 2005, pp. 329-332.

[20] Y. Wang, J. A. Henry, D. Sengupta, and M. A. Hines, *Appl. Phys. Lett.,* vol. 85, pp. 5736-5738, 2004.

[21] V. Bottom, *Introduction to Quartz Crystal Unit Design*. New York: Van Nostrand Reinhold Company, 1982.

[22] X. Liu, S. Morse, J. F. Vignola, D. M. Photiadis, A. Sarkissian, M. H. Marcus, and B. H. Houston, *Appl. Phys. Lett.,* vol. 78, pp. 1346-1348, 2001.

[23] M. Pandey, R. Reichenbach, A. Zehnder, A. Lal, and H. Craighead, in *NEMS '07. 2nd IEEE International Conference.*, 2007, pp. 880-885.

[24] Y.-H. Park and K. C. Park, *IEEE JMEMS,* vol. 13, pp. 238-247, 2004.

[25] Y.-H. Park and K. C. Park, *IEEE JMEMS,* vol. 13, pp. 248-257, 2004.

[26] M. C. Cross and R. Lifshitz, *Physical Review B,* vol. 64, pp. 1-22, 2001.

[27] Z. Hao, A. Ebril, and F. Ayazi, *Sensors and Actuators A,* vol. 109, pp. 156-164, 2003.

[28] Z. Hao and F. Ayazi, *Sensors and Actuators A,* vol. 134, pp. 582-593, 2007.

[29] J. Judge, D. M. Photiadis, J. F. Vignola, B. H. Houston, and J. Jarzynski, *Journal of Applied Physics,* vol. 101, pp. 013521-013521-11 2007.

[30] Y.-H. Cho, A. P. Pisano, and R. T. Howe, *JMEMS,* vol. 3, pp. 81-87, June 1994 1994.

[31] P. Y. Kwok, M. S. Weinberg, and K. S. Breuer, *JMEMS,* vol. 14, pp. 770-781, August 2005 2004.

[32] J. J. Blech, *J. of Lubrication Technology,* vol. 105, pp. 615-620, 1983.

[33] W. S. Griffin, H. H. Richardson, and S. Yamanami, *ASME Journal of Basic Engineering,* pp. 451-6, June, 1966 1966.

[34] T. Veijola, H.Kuisma, J. Lahdenppera, and T. Ryhanen, *Sensors and Actuators A,* vol. 48, pp. 239-248, 1995.

[35] T. Veijola and T. Mattila, in *Transducers '01*, Munchen, Germany, 2001, pp. 1506-9.

[36] E. Arkillic and K. S. Breuer, *JMEMS,* vol. 6, pp. 167-178, 1997 1997.

[37] A. Burgdorfer, *Journal of Basic Engineering,,* vol. 81, pp. 94-99, 1959 1959.

[38] M. N. Kogan, *Rarefied Gas Dynamics*. New York: Plenum Press, 1969.

[39] T. Veijola and A. Lehtovuori, "Numerical and compact modelling of squeeze-film damping in RF MEMS resonators," in *Proceedings of DTIP 2008* Nice, 2008, pp. 236-241.

[40] M. Weinberg, C. Dube, A. Petrovich, and A. Zapata, *JMEMS,* vol. 12, pp. 567-576, Oct. 5, 2003 2003.
[41] K. Yum, Z. Wang, A. Suryavanshi, and M.-F. Yu, *Journal of Applied Physics,* vol. 96, pp. 3933-3938, 2004.
[42] M. Weinberg, C. Dube, A. Petrovich, and A. Zapata, *IEEE JMEMS,* vol. 12, pp. 567-576, 2003.
[43] M. Martin, B. H. Houston, J. Baldwin, and M. Zalalutdinov, *IEEE JMEMS,* vol. 17, pp. 503-511, 2008.
[44] Y.-H. Cho, A. P. Pisano, and R. T. Howe, *IEEE JMEMS,* vol. 3, pp. 81-87, 1994.
[45] M. A. Varghese, R.; Sauer, D.; Senturia, S.D., in *Solid State Sensors and Actuators, 1997. TRANSDUCERS '97*, 1997, pp. 1121-1124 vol.2.
[46] S. A. Bhave, D. Gao, R. Maboudian, and R. T. Howe, *IEEE International Conference on MEMS,* pp. 223-226, 2005.
[47] K. Ekinci and M. L. Roukes, *Rev. of Sci. Instrum.,* vol. 76, p. 061101, 2005.
[48] D. Carr, S. Evoy, L. Sekaric, H. Craighead, and J. Parpia, *Appl. Phys. Lett.,* vol. 75, pp. 920-922, 1999.
[49] J. Yang, T. Ono, and M. Esashi, *IEEE JMEMS,* vol. 11, pp. 775-783, 2002.
[50] J. Henry, Y. Wang, D. Sengupta, and M. Hines, *J. Phys. Chem. B,* vol. 111, pp. 88-94, 2007.
[51] P. Mohanty, D. Harrington, K. Ekinci, Y. Yang, M. Murphy, and M. L. Roukes, *Physical Review B,* vol. 66, p. 085416, 2002.
[52] J. Henry, J. Wang, and M. Hines, *Appl. Phys. Lett.,* vol. 84, pp. 1765-1767, 2004.
[53] R. Mihailovich and N. MacDonald, *Sensors and Actuators A,* vol. 50, pp. 199-207, 1995 1995.
[54] J. Yang, T. Ono, and M. Esashi, *Appl. Phys. Lett.,* vol. 77, pp. 3860-3862, 2000.
[55] D. Wang, T. Ono, and M. Esashi, *Nanotechnology,* vol. 15, pp. 1851-1854, 2004.
[56] B. E. White and R. O. Pohl, in *Mat. Res. Soc. Symp. Proc.*, 1995, pp. 567-572.
[57] W. A. Phillips, *J. Low Temp. Phys.,* vol. 7, pp. 351-360, 1972.
[58] C. Seoánez, F. Guinea, and A. Castro Neto, *Phys. Rev. B,* p. 125107, 2008.
[59] D. Photiadis, in *Phonons 2007*, 2007, p. 012056.
[60] J. A. Geen and D. W. Carow, "Micromachined Gyros," US: Analog Devices, 2003.
[61] B. R. Johnson and M. W. Weber, "Mems Gyroscope with Horizontally Oriented Drive Electrodes," 2006.
[62] M. Weinberg and A. Kourepenis, *JMEMS,* vol. 15, pp. 479-491, June, 2006 2006.
[63] S. Lee and C. T. C. Nguyen, in *Solid-state Sensor and Actuator Workshop*, 2004, pp. 33-36.
[64] M. Agarwal, K. Park, M. Hopcroft, R. N. Candler, B. Kim, R. Melamud, G. Yama, B. Murmann, and T. W. Kenny, in *IEEE MEMS 06*, 2006.
[65] J. R. Vig and K. Yoonkee, *Ultrasonics, Ferroelectrics and Frequency Control, IEEE Transactions on,* vol. 46, pp. 1558-1565, 1999.
[66] L. Lin, R. T. Howe, and A. P. Pisano, *IEEE JMEMS,* vol. 7, pp. 286-294, 1998.
[67] R. N. Candler, A. Duwel, M. Varghese, S. A. Chandorkar, M. A. Hopcroft, P. Woo-Tae, K. Bongsang, G. Yama, A. Partridge, M. Lutz, and T. W. Kenny, *Microelectromechanical Systems, Journal of,* vol. 15, pp. 927-934, 2006.
[68] H. J. R. Abdolvand, G. K. Ho, A. Erbil, and F. Ayazi, *Microelectromechanical Systems, Journal of,* vol. 15, pp. 471 - 478 2006-06-05 2006.
[69] V. Kaajakari, T. Mattila, A. Oja, and H. Seppa, *Microelectromechanical Systems, Journal of,* vol. 13, p. 715, 2004.
[70] S. J. Wong, C. H. J. Fox, and S. McWilliam, *Journal of Sound and Vibration,* vol. 293, pp. 266-285, 2006.
[71] B. H. Houston, D. M. Photiadis, M. H. Marcus, J. A. Bucaro, X. Liu, and J. F. Vignola, *Applied Physics Letters,* vol. 80, pp. 1300-1302, 2002.
[72] A. Duwel, R. N. Candler, T. W. Kenny, and M. Varghese, *IEEE JMEMS,* vol. 15, pp. 1437-1445, 2006.
[73] "ANSYS®Academic Research," 11.0 ed.
[74] R. Lifshitz and M. L. Roukes, *Physical Review B,* vol. 61, p. 5600, 2000.
[75] S. Vengallatore, *Journal of Micromechanics and Microengineering,* vol. 15, pp. 2398-2404, 2005.
[76] J. E. Bishop and V. K. Kinra, *Journal of Reinforced Plastics and Composites,* vol. 12, pp. 210-226, February 1, 1993 1993.
[77] W. Jing, J. E. Butler, T. Feygelson, and C. T. C. Nguyen, in *Micro Electro Mechanical Systems, 2004. 17th IEEE International Conference on. (MEMS)*, 2004, pp. 641-644.
[78] W. Jing, Z. Ren, and C. T. C. Nguyen, *Ultrasonics, Ferroelectrics and Frequency Control, IEEE Transactions on,* vol. 51, pp. 1607-1628, 2004.
[79] L. Khine, M. Palaniapan, and W. Wai-Kin, in *Solid-State Sensors, Actuators and Microsystems Conference, 2007. TRANSDUCERS 2007. International*, 2007, pp. 2445-2448.
[80] D. Weinstein and S. A. Bhave, in *Electron Devices Meeting, 2007. IEDM 2007. IEEE International*, 2007, pp. 415-418.

[81] J. Wang, J. E. Butler, T. Feygelson, and C. T. C. Nguyen, in *IEEE 17th International Conference on MEMS*, 2004, pp. 641- 644.
[82] I. Wilson-Rae, *Physical Review B,* vol. 77, p. 245418, 2008.
[83] B. Li, H. Wu, C. Zhu, and J. Liu, *Sensors and Actuators A,* vol. 77, pp. 191-194, 1999.
[84] M. Bao, H. Yang, Y. Sun, and P. J. French, *J. Micromech. Microeng.,* vol. 13, pp. 795-800, 2003.
[85] X. Wang, M. Judy, and J. White, in *IEEE15th International Conference on MEMS*, 2002, pp. 210-213.
[86] J. Starr, in *IEEE Solid State Sensor and Actuator Workshop*, Hilton Head Island, SC, 1990, pp. 44-47.
[87] S. Hutcherson and W. Ye, *IOP Journal of Micromechanics and Microengineering,* vol. 14, pp. 1726-1723, 2004.
[88] P. Y. Kwok, M. S. Weinberg, and K. S. Breuer, *IEEE JMEMS,* vol. 14, pp. 770-781, 2005.
[89] Y.-J. Yang and C.-J. Yu, "Macromodel extraction of gas damping effects for perforated surfaces with arbitrarily-shaped geometries," in *Proc. MSM*, 2002, pp. 178-181.
[90] R. G. Christian, *Vacuum,* vol. 16, pp. 175-178, 1966.
[91] Z. Kadar, W. Kindt, A. Bossche, and J. Mollinger, *Sensors and Actuators A,* vol. 53, pp. 299-303, 1996.
[92] F. Blom, S. Bouwstra, M. Elwenspoik, and J. Fluitman, *Journal of Vacuum Science and Technology,* vol. 10, pp. 17-26, 1992.
[93] H. Hosaka, K. Itao, and S. Kuroda, *Sensors and Actuators A,* vol. 49, pp. 87-95, 1995.
[94] X. Liu, J. F. vignola, H. Simpson, B. Lemon, B. H. Houston, and D. M. Photiadis, *Journal of Applied Physics,* vol. 97, p. 023524 2005.
[95] A. Tewary, K. Yasumura, T. Stowe, and T. W. Kenny, in *Solid-state Sensor, Actuator, and Microsystems Workshop*, Hilton Head Island, SC, 2002, pp. 37-341.
[96] K. Wang, A. Wong, W. Hsu, and C. T. C. Nguyen, in *IEEE International Conference on Solid-state Sensors and Actuators*, Chicago, 1997, pp. 109-112.
[97] A. Duwel, M. Weinstein, J. Gorman, J. Borenstein, and P. Ward, in *IEEE 15th International Conference on MEMS*, 2002, pp. 214-219.

CONTACT

- Amy Duwel, aduwel@draper.com

[i] The cantilever dimensions are assumed to be of length L, width in the wafer plane w, thickness t, and surface layer thickness δ. The cantilever is assumed to sit on a semi-infinite support, except in the 3D analysis of [30], where a finite substrate thickness, h, is defined, and in squeeze-film damping where a gap to the substrate, g, is defined. Physical parameters include: E=elastic modulus, E_{sI} = imaginary (viscous) component of elastic modulus for a surface layer, ρ=density, C_{sp}=Specific heat capacity, α=CTE, K= thermal conductivity, γ=Grüneisen's constant τ_s=crystalline thermal time constant (=radius^2 $\rho C_{sp}/K$), τ_{ph}=phonon relaxation time, T=temperature , μ=viscosity of surrounding gas, P_o=pressure of surrounding gas. Also, c=speed of sound in solid, dC/dz=change in cantilever's readout capacitance with out-of-plane motion, m=cantilever mass, A_g= amplifier gain, and V_B=voltage bias across readout capacitance.